Effect of the Solvent Environment on the Spectroscopic Properties and Dynamics of the Lowest Excited States of Carotenoids

ARTICLE · MAY 2000

DOI: 10.1021/jp000079u

8 AUTHORS, INCLUDING:

James A Bautista

25 PUBLICATIONS **1,315** CITATIONS

SEE PROFILE

David Gosztola

Argonne National Laboratory

130 PUBLICATIONS **4,696** CITATIONS

SEE PROFILE

Effect of the Solvent Environment on the Spectroscopic Properties and Dynamics of the Lowest Excited States of Carotenoids

Harry A. Frank,*,† James A. Bautista,† Jesusa Josue,† Zeus Pendon,† Roger G. Hiller,‡ Frank P. Sharples,‡ David Gosztola,§ and Michael R. Wasielewski§,||

Department of Chemistry, University of Connecticut, Storrs, Connecticut 06269-3060, Department of Biological Sciences, Macquarie University, New South Wales 2109, Australia, Chemistry Division, Argonne National Laboratory, Argonne, Illinois 60439, and Department of Chemistry, Northwestern University, Evanston, Illinois 60208

Received: January 6, 2000; In Final Form: February 16, 2000

The spectroscopic properties and dynamics of the lowest excited singlet states of peridinin, fucoxanthin, neoxanthin, uriolide acetate, spheroidene, and spheroidenone in several different solvents have been studied by steady-state absorption and fast-transient optical spectroscopic techniques. Peridinin, fucoxanthin, uriolide acetate, and spheroidenone, which contain carbonyl functional groups in conjugation with the carbon−carbon π-electron system, display broader absorption spectral features and are affected more by the solvent environment than neoxanthin and spheroidene, which do not contain carbonyl functional groups. The possible sources of the spectral broadening are explored by examining the absorption spectra at 77 K in glassy solvents. Also, carotenoids which contain carbonyls have complex transient absorption spectra and show a pronounced dependence of the excited singlet state lifetime on the solvent environment. It is postulated that these effects are related to the presence of an intramolecular charge transfer state strongly coupled to the S_1 (2^1A_g) excited singlet state. Structural variations in the series of carotenoids studied here make it possible to focus on the general molecular features that control the spectroscopic and dynamic properties of carotenoids.

Introduction

The photochemical properties of carotenoids are determined in large part by the extents of their π-electron conjugation and the nature of functional groups attached to the conjugated chain.[1,2] These structural features determine the energies of their electronic transitions and also help position the molecules in the pigment−protein complexes of photosynthetic organisms. The structures, geometries, and interactions of carotenoids with the protein and with other pigments are important factors that control the mechanism and efficiency with which carotenoids carry out light-harvesting and photoprotection in vivo.[3,4]

Peridinin and fucoxanthin are two highly substituted carotenoids (Figure 1) that are among the most abundant found in nature.[5−7] Large amounts of peridinin are found in oceanic dinoflagellates, and of the roughly 1×10^7 tons per year of algal carotenoids produced in the oceans, fucoxanthin comprises approximately 60%, making it the most abundant carotenoid in the world.[5] Peridinin and fucoxanthin in vitro and in pigment−protein complexes have been studied by several research groups.[8−14] Both molecules are extremely efficient at harvesting light in photosynthetic organisms, having carotenoid-to-Chl energy transfer efficiencies approaching 100%.[5,6,9,15,16] Uriolide acetate (Figure 1) is a carotenoid found in a few species of marine algae, but little is known about its energy transfer capability.[17] Neoxanthin (Figure 1) is found in flowers, fruits, mosses, and the major light-harvesting pigment−protein complexes of green plants.[5] Spheroidene and spheroidenone (Figure 1) are the major carotenoids present in the bacterial species *Rhodobacter sphaeroides*.[5,18,19]

From extensive spectroscopic investigations of polyenes and carotenoids, it is now generally accepted that the characteristic strong absorption in the visible spectral region (Figure 2) of these molecules is attributable to an electronic transition between the ground state, S_0, which has A_g symmetry in the idealized C_{2h} point group, and a higher excited singlet, denoted S_2, which has B_u symmetry. Electronic transitions between S_0 and the first excited, S_1, state are optically forbidden because both S_0 and S_1 have the same (A_g) symmetry. The strong absorption in the visible region characteristic of all polyenes and carotenoids is associated with the $S_0 \rightarrow S_2$ ($1^1A_g \rightarrow 1^1B_u$) transition.

The wavelength of the maximum of the $S_0 \rightarrow S_2$ ($1^1A_g \rightarrow 1^1B_u$) absorption of carotenoids in the visible region is strongly affected by the solvent. Dispersion interactions between the solvent environment and the large transition dipole moment associated with this transition can significantly shift the spectral profiles.[20−23] For nonpolar carotenoids in nonpolar solvents, the magnitude of this effect has been shown to depend linearly on solvent polarizability.[20−23] The energy and dynamics of the $S_1 \rightarrow S_0$ ($2^1A_g \rightarrow 1^1A_g$) transition of carotenoids are not as strongly affected by changes in the solvent because the dipole moment associated with this transition is very small.[24] $S_1 \rightarrow S_0$ ($2^1A_g \rightarrow 1^1A_g$) solvent shifts are on the order of ~10% of those associated with the $S_0 \rightarrow S_2$ ($1^1A_g \rightarrow 1^1B_u$) transition.[1] Peridinin, unlike most other carotenoids, however, exhibits a pronounced solvent effect on the lifetime of its lowest excited singlet state.[25] The spectroscopic behavior and dynamics of peridinin in several different solvents have been examined by steady-state absorption, fluorescence, and fast-transient optical spectroscopy.[25] The

* To whom correspondence should be addressed. E-mail: frank@uconnvm.uconn.edu.
† University of Connecticut.
‡ Macquarie University.
§ Argonne National Laboratory.
|| Northwestern University.

10.1021/jp000079u CCC: $19.00
Published on Web 04/04/2000

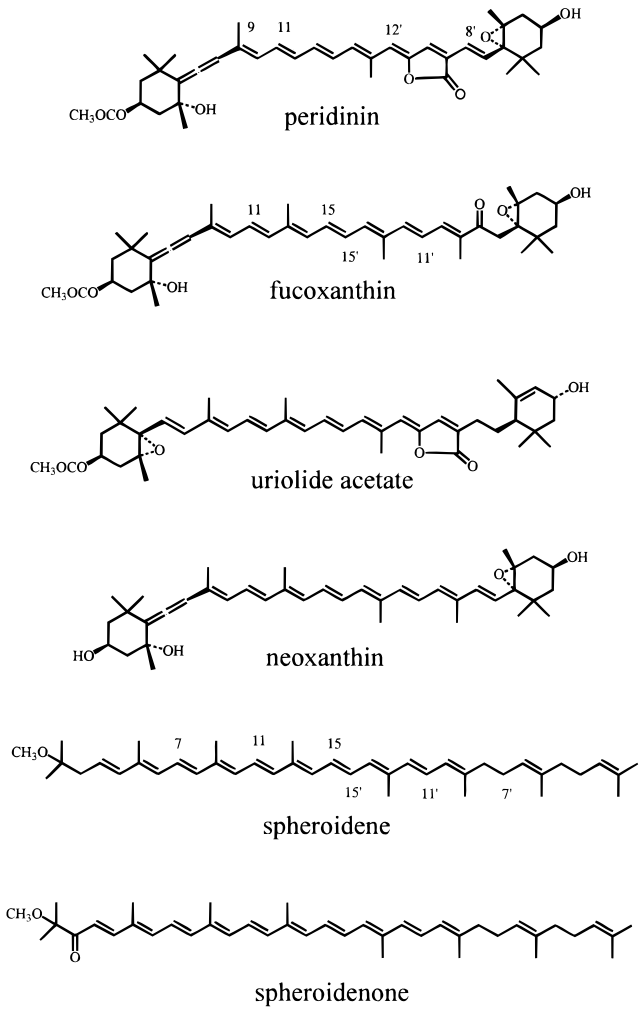

Figure 1. Molecular structures of the carotenoids used in the study.

lifetime of the lowest excited singlet state of peridinin was found to correlate strongly with solvent polarity, but not with polarizability. Moreover, hydrogen bonding of the solvent to peridinin was not an important factor in controlling the dynamics of the lowest excited singlet state.[25] The wavelengths of maximum fluorescence emission, the quantum yields of fluorescence, and the transient absorption spectra were also affected by the solvent environment.[25] A model explaining these data invoked the presence of an intramolecular charge transfer state in the excited-state manifold of peridinin.[9] It was suggested that the charge transfer state resulted from the presence of the lactone ring in the π-electron conjugation of peridinin. Analogous findings on aminocoumarins which also have lactone rings have been reported.[26]

In this work we explore the spectroscopic and dynamic behavior of peridinin, fucoxanthin, uriolide acetate, neoxanthin, spheroidene, and spheroidenone (Figure 1), in an attempt to elucidate the molecular features responsible for the dependence of the spectral properties and dynamics of some of these molecules on the solvent environment. Peridinin is a highly substituted, nor-carotenoid possessing a C_{37} carbon skeleton rather than the typical C_{40} system.[27] Peridinin, fucoxanthin, and neoxanthin possess an allene functional group in conjugation with the π-electron system, but peridinin is one of only a few carotenoids that contains a lactone ring. Fucoxanthin and neoxanthin do not have lactone rings, but fucoxanthin possesses a carbonyl functional group. Uriolide acetate possesses a lactone ring, but it lacks the allene group. Spheroidenone does not possess an allene group, nor does it have rings, but it does have a carbonyl group in the π-electron conjugated system. Spheroidene does not have rings, carbonyl, or allene. From an analysis of the spectral properties and dynamics of this systematic series of molecules, insight into those molecular features of carotenoids that control their photochemical behavior in vitro and in vivo can be obtained.

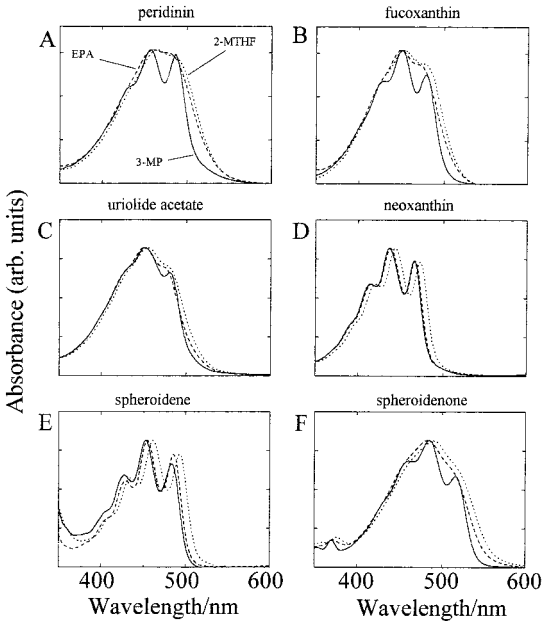

Figure 2. Absorption spectra of the carotenoids at room temperature in the solvents 3-MP (solid line), EPA (dashed line), and 2-MTHF (dotted line) which are representative of spectra in increasingly polar solvents. The spectra were normalized to the same relative maximum absorbance. The approximate absorbance of all the samples was 1.0 OD in a 1 cm path.

Materials and Methods

Sample Preparation. Peridinin was extracted from the peridinin−chlorophyll *a*−protein (PCP) complex and purified as previously described.[9] Fucoxanthin was extracted from the algae *Phaeodactylum tricornutum* which was cultured in Provasoli's enriched seawater medium at 18 °C under fluorescent light at an intensity of 20 μmol/m^2/s. Late log phase cells were harvested by centrifugation at 2000*g* and resuspended in a small volume of culture medium. Total pigments were extracted into *sec*-butanol as described by Martinson and Plumley[28] and purified in two steps using a Waters 996 high-performance liquid chromatograph (HPLC) employing a Nova-Pak C18 column. The first step utilized an acetone−methanol−water solvent system with the mobile phase programmed as follows: 0−10 min, isocratic 50% acetone/17% methanol/25% water; 10−30 min, linear gradient to 60% acetone/20% methanol/20% water; 30−60 min, linear gradient to 75% acetone/20% methanol/5% water. Fractions containing fucoxanthin were collected and reinjected into the HPLC machine using a two-solvent gradient protocol. Solvent A was 50% methanol/50% acetonitrile, and solvent B was 50% water/50% solvent A. The column was equilibrated with 20% A. The mobile phase was then programmed as follows: 0−5 min, isocratic 20% A; 5−15 min, linear gradient to 90% A; 15−40 min, linear gradient to 99% A. In both steps, the flow rate was 1 mL/min and the eluant was monitored at 440 nm. Fractions containing fucoxanthin were dried using a gentle stream of gaseous nitrogen in the dark. Uriolide acetate, a gift from Professor Synnøve Liaaen-Jensen, was purified using the protocol for fucoxanthin.

Spheroidene and spheroidenone were extracted from whole cells of *Rh. sphaeroides* 2.4.1 grown anaerobically and aerobically, respectively. A 150 mL sample of methanol and 20 mL of acetone were added to approximately 5 g of wet-packed cells and shaken until a dark green solution was obtained. The pigments were extracted using 100 mL of petroleum ether and loaded onto an alumina column preequilibrated with petroleum ether. A gradient of 0.5−4% ethyl acetate in petroleum ether was passed onto the column, and the carotenoid fractions were collected and dried by a gentle stream of nitrogen in the dark. The fractions were redissolved in acetone and injected into the HPLC machine with the mobile phase programmed as follows: 0−12 min, isocratic methanol/acetonitrile (95/5 v/v); 12−27 min, linear gradient to methanol/*n*-hexane (95/5 v/v); 27−45 min, linear gradient to methanol/acetonitrile (95/5 v/v). Major peaks containing the carotenoid of interest were collected and dried as described earlier.

Neoxanthin was extracted from spinach using approximately 200 g of young leaves that were ground and mixed with ∼500 mL of a 70/30 v/v acetone/methanol mixture. The mixture was filtered, and the acetone/methanol was evaporated on a rotary evaporator. The remaining residue was redissolved in ∼10 mL of a 90/10 v/v methanol/diethyl ether mixture and saponified in the dark, overnight, at room temperature, under nitrogen, using 6% w/v KOH. The saponified mixture of carotenoids was then extracted using diethyl ether, dried, and redissolved in acetone. Aliquots of this solution were then injected into the HPLC described above using a two-component (A and B) mobile phase where A = 9/1 v/v acetonitrile/water with 0.1% triethylamine and B = ethyl acetate. The run was programmed as follows: 0−16 min, linear gradient from 100% to 40% A; 16−40 min, isocratic 40% A. The flow rate was 1.0 mL/min. The fraction containing neoxanthin appeared at a retention time of approximately 8 min and was collected and dried in the dark using a gentle stream of gaseous nitrogen.

Solvents. The solvents used in this study were *n*-hexane, carbon disulfide, benzyl alcohol, isopentane, 3-methylpentane (3-MP), and 2-methyltetrahydrofuran (2-MTHF) from Aldrich, ethyl acetate, tetrahydrofuran, acetonitrile, and methanol (MeOH) from Fisher, pyridine, from Baker, and ethanol from AAPER. All of the solvents had a purity of >99.8%. EPA consisted of a mixture of diethyl ether, isopentane, and ethanol (5/5/2 v/v/v).

Spectroscopic Methods. Steady-State Absorption. Absorption spectra were recorded at room temperature and 77 K using a Milton Roy Spectronic 3000 photodiode array spectrometer.

Time-Resolved Optical Spectroscopy. Transient absorption data were obtained with a regeneratively amplified Ti:sapphire laser described previously.[29,30] The system furnishes 140 fs transform-limited pump pulses that are tunable from 470 to 820 nm. Typically 0.3−1 mJ was used to excite the molecules, and the spectral profiles were probed using a white light continuum generated by appropriate beam splitters passing part of the pump beam through a sapphire window.

Computational Methods. Spectral Deconvolutions. The absorption spectra were deconvolved into a sum of Gaussian components using Origin version 6.0 software.[31] Starting values of the vibronic bands in wavenumbers were taken from the locations of the peaks and shoulders in the experimental spectra, and incorporated the assumption that the spacings of the vibrational peaks should be roughly equidistant. In the first calculation, the parameters of position, width, area, and spacing were allowed to vary using a maximum of 100 iterations of the Levenberg−Marquardt algorithm. Constraints were then imposed on the widths of the Gaussians so that each vibronic band was less than double the width of an adjacent band and with the baseline set to a constant value. Finally, locations of the peaks were fixed by the above calculations, and only the widths and areas of adjacent and nonadjacent Gaussians were allowed to vary, keeping all other parameters constant.

Dipole Moment Calculations. The ground-state dipole moments of the molecules were calculated using a Gateway Performance 500 computer (500 MHz, 384 MB RAM) running Hyperchem version 5.11 software.[32] Geometries of the carotenoids were fully optimized using the MM+ force field molecular mechanics methods contained in Hyperchem followed by a semiempirical molecular orbital computation using the AM1 Hamiltonian and the Polak−Ribiere minimization method.

Results

Absorption Spectra. Room temperature absorption spectra of peridinin, fucoxanthin, uriolide acetate, neoxanthin, spheroidene, and spheroidenone in 3-MP, EPA, and 2-MTHF, which are representative of spectra in increasingly polar solvents, are shown in Figure 2. In general, the spectra are characterized by intense, broad (fwhm ≈ 4000−5000 cm^{-1}) bands in the 350−550 nm region known to be associated with $S_0 \rightarrow S_2$ transitions. In the nonpolar solvent, 3-MP, the absorption bands of all of the carotenoids show resolved vibronic structure with the longest wavelength feature corresponding to the spectral origin. The resolution of the vibronic structure in the spectra of peridinin, fucoxanthin, uriolide acetate, and spheroidenone decreases dramatically when the molecules are dissolved in the more polar solvents 2-MTHF and EPA. In addition to losing vibronic structure in the more polar solvents, the widths of the absorption bands increase (Figure 2A−C,F). In neoxanthin and spheroidene, the resolution in the vibronic bands and the widths of the absorption spectra are not affected by changes in the polarity of the solvent. (See Figures 2D,E.) Small shifts in their vibronic peak positions can be attributed to changes in the polarizability of the medium.[20−23] Theoretical models of the solvatochromic effect on the absorption spectra of nonpolar molecules in nonpolar solvents explain the linear relationship between band position and $R(n)$, the polarizability factor. ($R(n) = (n^2 - 1)/(n^2 + 2)$, where n is the index of refraction of the solvent.[1,23]) For peridinin, the maxima of the absorption spectra in various polar solvents do not correlate in a linear manner with solvent polarizability.[25]

Absorption spectra of peridinin, fucoxanthin, spheroidene, and spheroidenone were also recorded in 77 K glasses of EPA and either 2-MTHF or 3-MP. The spectra are displayed in Figure 3, where they have been converted from the fixed band-pass wavelength absorption experiment to a wavenumber scale by multiplying the spectral intensities by the square of the wavelength.[33] The spectral line shapes were then deconvolved into Gaussian components (Figure 3). The fitting parameters are summarized in Table 1. In all of the $S_0 \rightarrow S_2$ spectra shown in Figure 3, lowering the temperature enhanced the resolution compared to that of absorption spectra taken at room temperature and shown in Figure 2.

Compared to the other molecules examined here, peridinin shows the most dramatic effect of solvent on its room temperature absorption spectrum. A closer analysis shows that the width of the absorption band depends strongly on the polarity of the solvent. If the bandwidth (fwhm) is plotted versus $P(\epsilon)$, the polarity function ($P(\epsilon) = (\epsilon - 1)/(\epsilon + 2)$ where ϵ is the dielectric constant of the solvent), it is seen to increase linearly to a point where $P(\epsilon) \approx 0.4$, which corresponds to a solvent

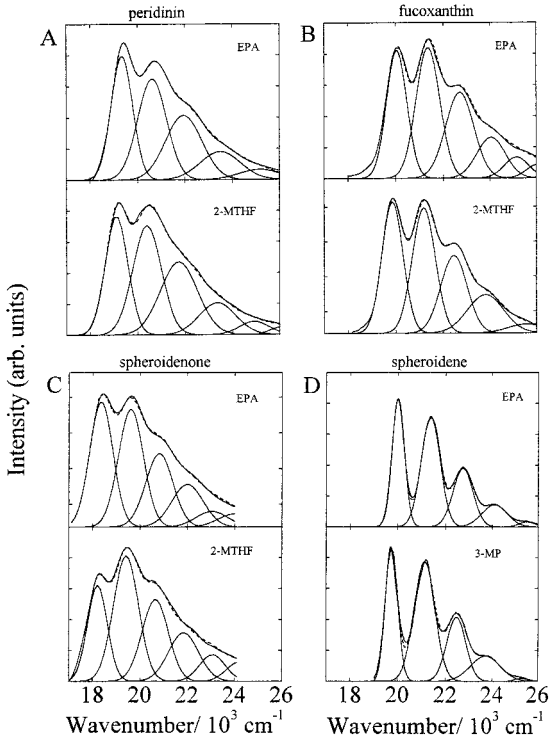

Figure 3. Absorption spectra of peridinin, fucoxanthin, spheroidene, and spheroidenone in 77 K glasses of EPA and 2-MTHF or 3-MP. The spectra were plotted on a wavenumber scale, and the intensity was mathematically corrected for the effect of transforming the data from the fixed band-pass wavelength scale experiment to a nonlinear band-pass wavenumber scale. The spectra were then analyzed by Gaussian deconvolution as described in the text. The dashed lines correspond to the fitted spectra.

dielectric constant, $\epsilon \approx 3.0$, and then shows no further significant change at values above that point (Figure 4).

The fluorescence emission spectra of peridinin, fucoxanthin, neoxanthin, and spheroidene have been published and will not be reproduced here.[9,25,34,35] However, it is worth mentioning that the fluorescence emission spectrum of uriolide acetate (data not shown) is very similar to the spectra of peridinin and fucoxanthin in that it is broad and substantially red-shifted relative to its absorption spectrum. The large Stokes shift between the emission and absorption suggests that its fluorescence, like that from peridinin and fucoxanthin, corresponds to an $S_1 \rightarrow S_0$ ($2^1A_g \rightarrow 1^1A_g$) transition rather than an $S_2 \rightarrow S_0$ ($1^1B_u \rightarrow 1^1A_g$) transition.[9,25] In contrast, the emission spectra of neoxanthin, spheroidene, and spheroidenone are not substantially red-shifted relative to their absorption spectra.[34] This indicates that the fluorescence from these carotenoids corresponds to an $S_2 \rightarrow S_0$ ($1^1B_u \rightarrow 1^1A_g$) transition rather than an $S_1 \rightarrow S_0$ ($2^1A_g \rightarrow 1^1A_g$) transition.

Dipole Moment Calculations. The dipole moments of peridinin, fucoxanthin, neoxanthin, uriolide acetate, spheroidene, and spheroidenone were calculated from their fully optimized geometries using an AM1 Hamiltonian. The results are summarized in Table 2, which show that peridinin and fucoxanthin have significantly larger ground-state dipole moments than the other molecules in the group. The calculation also shows that peridinin has a substantial projection of its dipole moment along the long axis of the conjugated π-electron chain, whereas the other molecules have smaller projections of their dipole moments along the polyene chain.

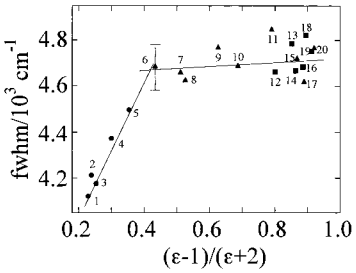

Figure 4. A plot of the bandwidth (fwhm) of the $S_0 \rightarrow S_2$ transition of peridinin vs the polarity function, $P(\epsilon) = (\epsilon - 1)/(\epsilon + 2)$, where ϵ is the dielectric constant of the solvent. The error in the points is approximately ± 100 cm^{-1} and is derived from the uncertainty in assigning the half-heights of the absorption bands. It is represented by the error bar on solvent data point 6 (propyl ether). The circles, triangles, and squares represent peridinin in nonpolar, polar, and hydrogen-bonding solvents, respectively. The solvent key is given in Table 3.

Transient Absorption Experiments. Excitation of the carotenoids into their strong visible absorption bands with a laser pump beam results in a rapid buildup of a transient absorption which decays rapidly with single-exponential kinetics as the excited singlet state is depopulated to the ground state. Representative decay traces for several carotenoids have been published.[9,35] Table 3 summarizes the results for the lifetimes of the lowest excited singlet states of peridinin, fucoxanthin, neoxanthin, uriolide acetate, spheroidene, and spheroidenone. The data show that, for peridinin, fucoxanthin, and uriolide acetate, the lifetimes depend on the solvent. The data for peridinin from Table 3 are plotted in Figure 5A and reveal that the lifetime is constant to a point where the solvent polarity function $P(\epsilon) = (\epsilon - 1)/(\epsilon + 2) \approx 0.4$; then at $P(\epsilon)$ values larger than 0.4, the lifetime decreases linearly with increasing solvent polarity.[25] For fucoxanthin, the lifetime is constant up to a $P(\epsilon)$ value of 0.6, after which point it decreases linearly. (See Figure 5B.) Uriolide acetate shows a similar effect of the solvent on the lifetime of the lowest excited singlet state. (See Figure 5C.) The dielectric threshold at which the lifetime of uriolide acetate starts to decrease is $P(\epsilon) \approx 0.6$. The lifetimes of the lowest excited states of neoxanthin, spheroidene, and spheroidenone show no dependence on the solvent environment (Table 3).

Transient absorption spectra of the carotenoids in the representative nonpolar and polar solvents, *n*-hexane and MeOH,

TABLE 1: Positions of Gaussian Band Maxima, $\bar{\nu}$, and Full Width at Half-Maximum, Δ, Values for Each of the Gaussian Components in the $S_0 \rightarrow S_2$ Absorption Spectra Taken at 77 K (cm^{-1})[a]

carotenoid	solvent	$\bar{\nu}_{0-0}$	Δ_{0-0}	$\bar{\nu}_{0-1}$	Δ_{0-1}	$\bar{\nu}_{0-2}$	Δ_{0-2}	$\bar{\nu}_{0-3}$	Δ_{0-3}	$\bar{\nu}_{0-4}$	Δ_{0-4}
peridinin	EPA	19 339	903	20 168	1222	21 954	1543	23 500	1700	25 157	1741
	2-MTHF	19 099	939	20 386	1207	21 734	1582	23 363	1531	24 912	1238
fucoxanthin	EPA	20 043	854	21 356	1000	22 701	1205	24 047	1226	25 147	1054
	2-MTHF	19 854	888	21 169	973	22 446	1130	23 800	1562	25 572	1577
spheroidenone	EPA	18 355	979	19 600	1052	20 804	1158	22 004	1333	23 037	1358
	2-MTHF	18 208	830	19 407	1055	20 643	1109	21 850	1280	23 073	1088
spheroidene	EPA	20 000	526	21 364	797	22 737	850	24 094	1099	25 500	700
	3-MP	19 734	527	21 126	873	22 472	802	23 716	1277	25 277	555

[a] The spectral traces are given in Figure 3.

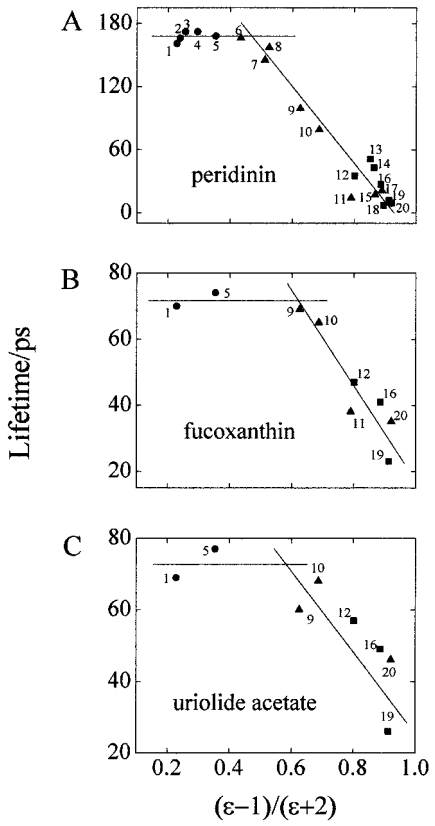

Figure 5. Lifetimes of the lowest excited singlet state of (A) peridinin, (B) fucoxanthin, and (C) uriolide acetate versus the solvent polarity function, $P(\epsilon) = (\epsilon - 1)/(\epsilon + 2)$. The lifetimes are constant up to a point where $P(\epsilon) \approx 0.4$ for peridinin and 0.6 for both fucoxanthin and uriolide acetate. The circles, triangles, and squares represent the molecules in nonpolar, polar, and hydrogen-bonding solvents, respectively. The numerical data and solvent key are given in Table 3. The uncertainties in the lifetimes are approximately ±10% for the values in the polar solvents and approximately ±5% for the values in the nonpolar solvents on the basis of the reproducibility of the measurements.

TABLE 2: Dipole Moments of the Ground States of the Carotenoids and the Projections of the Dipole Moments along the Conjugated π-Electron Chain[a]

carotenoid	$\lvert\vec{\mu}\rvert$	cos θ	carotenoid	$\lvert\vec{\mu}\rvert$	cos θ
peridinin	5.7	0.88	neoxanthin	2.1	0.10
fucoxanthin	8.8	0.39	spheroidene	1.7	0.56
uriolide acetate	2.6	0.31	spheroidenone	1.5	0.17

[a] The magnitudes of the dipole moments are given in debyes. θ corresponds to the angle between the direction of the dipole moment and the long axis of the polyene chain defined as a vector connecting carbons 11 and 11′ in the carotenoid.

respectively, are shown in Figure 6. At least two bands are evident in the spectrum of peridinin in *n*-hexane and in the spectra of fucoxanthin, uriolide acetate, and spheroidenone in *n*-hexane and MeOH (Figure 6A−C,F). There is only one transition evident in the spectra of neoxanthin and spheroidene, and essentially no dependence on solvent polarity for these molecules is observed. The most dramatic solvent effect is seen for peridinin (Figure 6A). In *n*-hexane one transient feature appears at ∼510 nm. The wavelength of this band has been shown in previous work to red shift as the solvent polarizability is increased,[25] and its intensity diminishes significantly as the polarity of the solvent is increased (Figure 6B). In the more polar solvent MeOH, this first band is barely noticeable as a small shoulder on the short-wavelength side of a second, much broader band appearing at ∼590 nm in the transient spectrum.

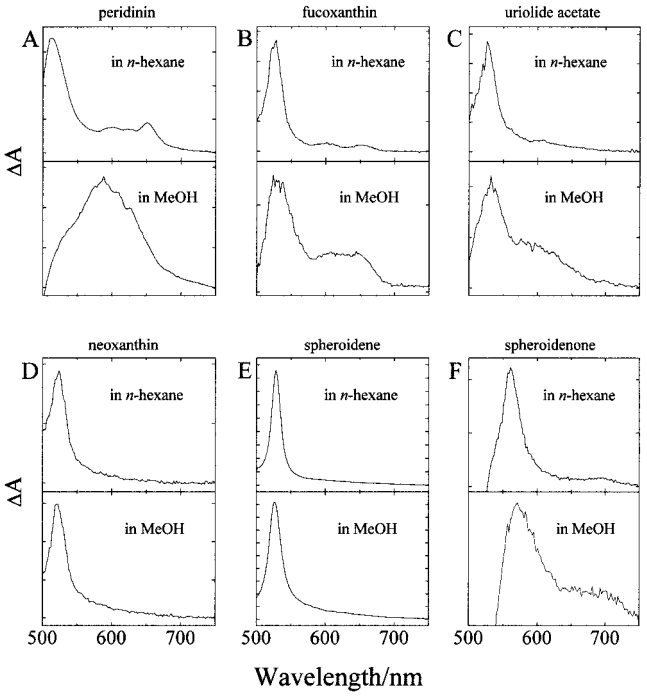

Figure 6. Transient absorption spectra of the carotenoids in *n*-hexane and methanol, representing nonpolar and polar environments, respectively. The optical densities of the samples were between 0.8 and 1.0 measured in a 1 cm cuvette at the excitation wavelength. The separation between tick marks on the ordinate axes of all the spectra corresponds to an absorbance change (Δ*A*) of 0.01 in the 2 mm path cell used for the transient experiments. The molecules were excited with 140 fs pulses at the red-most vibronic feature of the ground-state absorption, and the transient spectra were recorded after a time delay of the probe beam corresponding to between 5% and 10% of the lifetime of the transient.

This second band shifts to ∼660 nm in the nonpolar solvent, *n*-hexane (Figure 1A). Similar effects, although not as dramatic, are seen in the transient spectra of fucoxanthin, uriolide acetate, and spheroidenone (Figure 6B,C,F). All three of these molecules display at least two characteristic bands in their transient absorption spectra. The first is a narrow feature, appearing between 500 and 600 nm, and the second is much broader, appearing between ∼600 and ∼700 nm. The ratio of the intensities of the first band to the second band decreases for all three of these molecules in going from the nonpolar solvent, *n*-hexane, to the polar solvent, MeOH.

Discussion

Spectral Broadening. There are two types of spectral broadening observed in these experiments. The first derives from the presence of a carbonyl substituent in conjugation with the π-electron system. This substituent-induced broadening is illustrated by comparing the room temperature absorption spectrum of spheroidene (Figure 2E) with that of spheroidenone (Figure 2F). The second type of broadening is induced by polar solvents; e.g., compare the absorption spectra of fucoxanthin (Figure 2B) in 3-MP and 2-MTHF. This solvent-induced broadening occurs only when substituent-induced broadening is present; e.g., compare the absorption spectra of neoxanthin (Figure 2D) in 3-MP and 2-MTHF. Neoxanthin has no carbonyl functional group in its conjugated π-electron system and shows essentially no solvent-induced broadening.

It is well-known that polyenes possessing C_{2h} symmetry have strongly allowed $S_0 \rightarrow S_2$ ($1^1A_g \rightarrow 1^1B_u$) and strongly forbidden $S_0 \rightarrow S_1$ ($1^1A_g \rightarrow 2^1A_g$) transitions.[1,24] Although the molecular structures of carotenoids deviate from this idealized symmetry

TABLE 3: Excited Singlet State Lifetimes, τ, of the Carotenoids in Various Solvents Having Different Polarity Factors, $P(\epsilon)$[a]

			τ/ps					
solvent	no.	$P(\epsilon)$	peridinin	fucoxanthin	uriolide acetate	neoxanthin	spheroidene	spheroidenone
n-hexane	1	0.229	161 ± 3	70 ± 2	69 ± 2	35 ± 2	8 ± 1	6 ± 1
n-heptane	2	0.239	166 ± 3	–	–	–	–	–
cyclohexane	3	0.256	172 ± 3	–	–	–	–	–
benzene	4	0.295	172 ± 3	–	–	–	–	–
carbon disulfide	5	0.354	168 ± 3	74 ± 2	77 ± 4	–	9 ± 1	6 ± 1
propyl ether	6	0.434	166 ± 3	–	–	–	–	–
1,2,4-trichlorobenzene	7	0.512	145 ± 3	–	–	–	–	–
diethyl acetate	8	0.526	157 ± 3	–	–	–	–	–
ethyl acetate	9	0.626	99 ± 3	69 ± 2	60 ± 2	–	8 ± 1	–
tetrahydrofuran	10	0.687	79 ± 2	65 ± 2	68 ± 2	–	8 ± 1	–
pyridine	11	0.790	14 ± 2	38 ± 2	–	–	9 ± 1	–
benzyl alcohol	12	0.801	35 ± 2	47 ± 2	57 ± 2	–	9 ± 1	–
2-propanol	13	0.852	51 ± 2	–	–	–	–	–
1-propanol	14	0.864	43 ± 2	–	–	–	–	–
acetone	15	0.868	17 ± 2	–	–	–	–	–
ethanol	16	0.886	27 ± 2	41 ± 2	49 ± 3	–	8 ± 1	–
benzonitrile	17	0.890	21 ± 3	–	–	–	–	–
2,2,2-trifluoroethanol	18	0.895	7 ± 1	–	–	–	–	–
methanol	19	0.913	12 ± 2	23 ± 2	26 ± 2	35 ± 2	8 ± 1	6 ± 1
acetonitrile	20	0.921	9 ± 1	35 ± 2	46 ± 2	–	8 ± 1	6 ± 1

[a] The transient absorbance decays were fit with single-exponential functions from which the lifetimes were derived. The table is sorted by the magnitude of the polarity factor, $P(\epsilon)$, which was determined from the dielectric constants for the solvents using the expression $P(\epsilon) = (\epsilon - 1)/(\epsilon + 2)$. A dash in the table means that the value was not measured.

(Figure 1), they tend to obey these selection rules. The highly substituted molecules, peridinin, fucoxanthin, uriolide acetate, and spheroidenone, challenge the strictness of these selection rules, however. In these molecules, it is possible that owing to the breakdown in symmetry, the $S_0 \rightarrow S_1$ transition may become more allowed and contribute to the overall absorption spectrum. Vibronic coupling between S_1 and S_2 precludes exact mirror-image symmetry between the $S_0 \rightarrow S_1$ absorption and $S_1 \rightarrow S_0$ emission transitions. However, a rough estimate of the position of the forbidden $S_0 \rightarrow S_1$ absorption can be obtained by reflecting the $S_1 \rightarrow S_0$ fluorescence spectra[9,13,25] (data not shown) about the spectral origin. The center of the $S_0 \rightarrow S_1$ absorption band is predicted to be very close to the spectral origin of the $S_0 \rightarrow S_2$ transition, where it would contribute to the experimentally observed absorption line shape. This might not be seen in the spectra of the less-substituted neoxanthin and spheroidene, which are expected to obey the selection rules more strongly.

An estimate of the allowedness of the $S_0 \rightarrow S_1$ absorption relative to the $S_0 \rightarrow S_2$ transition can be obtained by comparing the radiative lifetimes of the S_1 and S_2 states. The radiative lifetime of the S_1 state can be obtained by dividing the lifetime of the state by the quantum yield of fluorescence. An example is peridinin in *n*-hexane, where these values are 161 ps and 8.7×10^{-4}, respectively,[25] and yield a value for the radiative lifetime of the S_1 state of 1.8×10^{-7} s. For the radiative lifetime, τ_0, of the S_2 state, the Strickler–Berg relationship[36]

$$k_r = 1/\tau_0 = (2.880 \times 10^{-9}) n^2 \frac{\int I(\nu)\, d\nu}{\int \nu^{-3} I(\nu)\, d\nu} (g_l/g_u) \int \epsilon(\nu)\, d \ln \nu$$

can be used. $I(\nu)$ and $\epsilon(\nu)$ are the fluorescence intensity and molar absorptivity, respectively, at the frequency ν (cm^{-1}). g_l and g_u are the degeneracies of the lower and upper states, and n is the refractive index of the medium. Using this relationship, τ_0 for the S_2 state of peridinin in *n*-hexane was calculated to be 2.0×10^{-9} s. Comparing this value to the radiative lifetime of the S_1 state indicates that the $S_0 \rightarrow S_1$ transition for peridinin in *n*-hexane is predicted to be 100 times less allowed than the $S_0 \rightarrow S_2$ transition, and consequently very difficult to observe.

To examine experimentally whether there is any evidence for $S_0 \rightarrow S_1$ absorption contributing to the overall line shape, the absorption spectra of peridinin, fucoxanthin, and spheroidenone were taken in 77 K glasses of EPA and either 2-MTHF or 3-MP, which enhanced the spectral resolution of the vibronic peaks. Gaussian deconvolutions of the spectra of peridinin, fucoxanthin, spheroidene, and spheroidenone are very similar (Figure 3). The narrowest band in all the spectra (the lowest energy Gaussian component) corresponds to the spectral origin. The spectrum of spheroidene is the best resolved of the group, but none of the deconvolutions are strikingly different (Figure 3, Table 1), nor do they require additional band(s) to fit the line shapes. In other words, the low-temperature absorption spectra show no evidence for $S_0 \rightarrow S_1$ absorption. The band shapes are easily accommodated by normal progressions of vibronic peaks associated with carbon–carbon chain stretching frequencies characteristic of polyene and carotenoid absorption spectra.[1]

Another possibility is that nπ^* states associated with the nonbonding electrons on the carbonyl oxygen couple with the S_2 (1^1B_u) state in a manner that leads to band broadening. There are many examples of broadening of absorption spectra of π-electron-conjugated molecules due to vibronic perturbation of $\pi\pi^*$ states with the vibrational electronic levels of nπ^* states.[37] However, the effects of the solvent on the dynamics of the lowest excited singlet and the broadening of the $S_0 \rightarrow S_2$ absorption spectra are not consistent with the involvement of nπ^* states. A major effect of low-lying nπ^* states is to enhance spin–orbit coupling with $\pi\pi^*$ triplet states.[38] This would increase the probability of intersystem crossing and shorten the lifetime of the lowest lying excited singlet state. Hydrogen bonding of a solvent molecule to the carbonyl oxygen of any of these carotenoids would be expected to stabilize the occupied n orbital and result in a shift of the nπ^* states to higher energy. Thus, the lifetimes of the first excited singlet states of these molecules would be predicted to become longer in hydrogen-bonding solvents, rather than shorter as observed here (Table 3). Also, the fact that the lifetime of the lowest excited singlet states of these molecules in the strongly polar non-hydrogen-bonding solvent, acetonitrile, is comparable to the lifetime in

hydrogen-bonding solvents is strong evidence that nπ^* states are not involved in determining the dynamics of the lowest excited singlet states. Furthermore, if nπ^* states were involved, one would expect the absorption spectra of the carotenoids to be broader in the nonpolar solvents where the nπ^* states are thought to be closest to the $\pi\pi^*$ states.[37] Precisely, the opposite is seen. The absorption spectra of the carotenoids are most highly resolved in nonpolar solvents (Figures 2 and 4).

Bublitz et al.[39,40] have carried out electroabsorption (Stark) spectroscopic experiments of donor/acceptor-substituted polyenes and discussed broadening of the absorption spectra with increasing solvent polarity. They have shown that, depending on the solvent, the *ground-state* structure of the solvated molecule can become more or less dipolar, depending on interactions with the matrix electric field. Changes in the dipole moment and polarizability of the molecules are observed and mirrored by shifts in the position and by broadening of absorption spectra. If the behavior of peridinin, fucoxanthin, uriolide acetate, and spheroidenone bears any resemblance to that of donor/acceptor polyenes, the carotenoids would be categorized as containing very weak donor/acceptor end groups. This is because there is no specific functional group or substituent, except the allene in peridinin and fucoxanthin, or the polyene chain itself, that can act as an electron donor. Also, the carotenoids here have carbonyls as electron acceptors. As described by Bublitz et al.[40] the relative strength of an electron acceptor can be approximated by the acidity of the end group free from the polyene chain. An end group consisting solely of a carbonyl substituent has a very high pK_a, suggesting that it is not a strong electron acceptor.

What then is the source of the substituent- and solvent-induced band broadening in the absorption spectra of peridinin, fucoxanthin, uriolide acetate, and spheroidenone compared to those of neoxanthin and spheroidene? The major difference between these groups of molecules is that peridinin, fucoxanthin, uriolide acetate, and spheroidenone have a carbonyl in their conjugated π-electron systems. Christensen and Kohler[41] addressed the issue of spectral diffuseness for retinal in rigid glasses at 77 K compared to simpler polyenes and apo-carotene analogues with roughly the same extent of π-electron conjugation. They suggested that band broadening could arise from (1) coupling of the S_2 (1^1B_u) state to spectroscopically undetectable states in proximity, (2) the presence of a congested manifold of strongly coupled vibronic lines, and/or (3) conformational disorder due to the presence of nonbonded interactions between the methyl groups along the conjugated chain and the β-ionylidene rings. These authors concluded that conformational disorder was a sufficient cause for spectral broadness of retinal and analogue molecules, but that additional contributions from the other sources could not be completely ruled out. The presence of β-ionylidene rings on polyenes can lead to a loss of resolution in the absorption spectra.[41] This is due to repulsion between the methyl groups on the β-ionylidene rings and a neighboring hydrogen atom at carbon 7 in the apo-carotenes.[1,41,42] An apparently shallow and flat potential surface associated with the dihedral bond angle for the carbons in this part of the molecule can result in an ensemble of conformational isomers having a broad range of effective π-electron conjugations. The collection of conformers would possess a distribution of transition energies that give rise to broad optical spectra in solution.[1]

The most likely interpretation for the substituent-induced spectral broadening observed from the carotenoids studied here is that, when the carbonyl group is present in conjugation with the carbon π-electron system, a wider distribution of conformational isomers is formed than when the steric repulsion is only between methyl groups and hydrogens. Additional flattening of the ground-state potential energy surface by interactions between the polar solvents and the polar carbonyl group can lead to further broadening of the spectra. This can occur up to a particular dielectric strength, at which point the broadening levels off without any further effect of solvent polarity (Figure 4). This may be an indication that the maximum in the statistical distribution of conformers has been reached, in which case no further change in the width of the absorption spectrum would be expected with increasing solvent polarity. The effect of solvent might also be less for the molecules that do not contain carbonyls because their dipole moments are generally smaller. The computed dipole moments of the ground state of peridinin and fucoxanthin are significantly larger than those of the other molecules in the series. (See Table 2.) Also, unlike the other molecules which show less or no broadening with solvent, peridinin has a large projection of its dipole moment along the polyene chain. This could enhance the conformational disorder, which leads to spectral broadening because the $S_0 \rightarrow S_2$ absorption transition dipole also lies along the polyene chain.

Effect of Solvent on the Excited-State Properties. It is observed that the dynamics of the excited singlet states of peridinin, fucoxanthin, and uriolide acetate are constant with increasing solvent polarity up to a certain dielectric threshold, which is different for the different molecules, and then decrease linearly beyond that point (Table 3 and Figure 5). The dependence of the dynamics on the dielectric strength of the solvent is suggestive of an electronic state that has a large dipole moment either in proximity to or coupled with the 1^1A_g state. Previously,[25] it was postulated that peridinin possesses a nonemissive charge transfer state, denoted S_{CT}, in its excited-state manifold of electronic states, and that this was responsible for the large effect of solvent polarity on the dynamics of its excited singlet state. It was hypothesized that the charge transfer state could be either a twisted intramolecular charge transfer (TICT) state or a nontwisted intramolecular charge transfer (ICT) state, whose energies are known to be highly susceptible to the solvent environment as demonstrated by experiments on aminocoumarins,[26] 4-(9-anthryl)-*N*,*N*-dimethylaniline (ADMA),[43] and related compounds.[44] In nonpolar solvents, the charge transfer state could be higher in energy than the 2^1A_g state, yet sufficiently close that it may be thermally populated after light absorption and fast relaxation from S_2 to either the charge transfer or 2^1A_g state. This would account for the observation of at least two electronic transitions in the transient spectral profile of peridinin in low dielectric media (Figure 6A). The shorter-wavelength, narrow band is observed in all known transient spectra from carotenoids and was assigned to an $S_1 \rightarrow S_n$ transition (e.g., see ref 45). The longer-wavelength, broader transition was assigned to the $S_{CT} \rightarrow S_{n'}$ component of the spectra because of its marked similarity to that from ADMA and other related compounds, which are attributable to these transitions.[26,43] Fucoxanthin, uriolide acetate, and spheroidenone in addition to peridinin (Figure 6A−C,F) display at least two electronic transitions in their transient spectral profiles and have a carbonyl in conjugation with the carbon−carbon double bond system. The electron-withdrawing character of this functional group is expected to help stabilize the charge transfer character of the configuration, especially in polar solvents. Spheroidene and neoxanthin show only a single narrow band in their transient spectral profiles, consistent with their lack of both a carbonyl

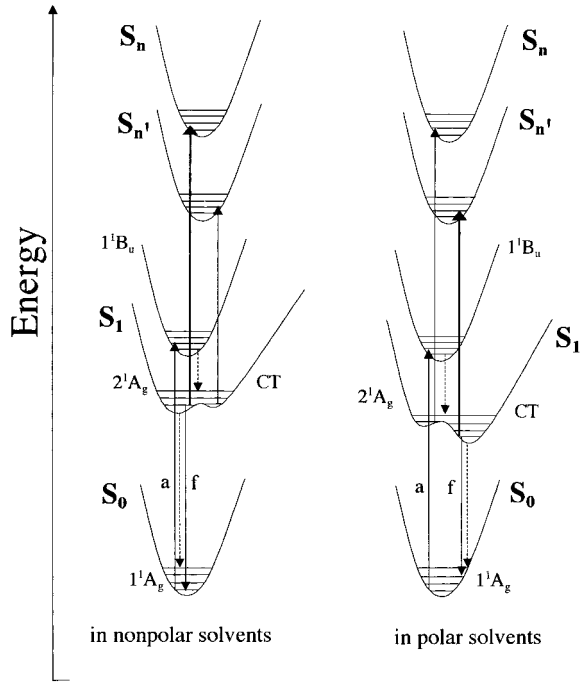

Figure 7. Potential energy surface diagram representing the effect of the solvent environment on peridinin, and to a lesser extent the other carbonyl-containing carotenoids. The left-hand figure represents the situation for the molecules in nonpolar solvents. On the right, the disposition of the states in polar solvents is represented. The S_1 state surface is comprised of two strongly coupled states, 2^1A_g and a CT state. The solid vertical lines represent radiative transitions, and the dashed vertical lines represent nonradiative transitions. The thickness of the lines representing the $S_1 \rightarrow S_n$ and $S_1 \rightarrow S_{n'}$ transitions is meant to represent qualitatively their relative intensities in the spectra shown in Figure 6. The model is based on several experimental observations described in the text. In increasingly polar solvents, the potential energy surface of the S_1 state is significantly distorted owing to mixing with a CT state. This alters both the positions of the transitions and dynamics of the lowest excited state.

functional group and significant charge transfer character in the excited state.

An energy level diagram that can be used to describe the excited-state dynamics and spectral behavior of the carotenoids is shown in Figure 7. The primary electronic transitions between the various singlet states for the molecules in nonpolar and polar solvents are represented separately. The model invokes strong mixing between an intramolecular charge transfer state (CT) and the 2^1A_g state that leads to a distorted S_1 excited-state potential energy surface whose energy minimum is solvent dependent. The figure is based primarily on the behavior of peridinin, which shows the most extreme effect of the solvent. However, the model can also be applied to the other carotenoids, but the distortion of the S_1 potential energy surface will be either less severe for fucoxanthin, uriolide acetate, and spheroidenone which contain carbonyls, or not at all for neoxanthin and spheroidene which do not contain carbonyls. The model is consistent with the following observations: (1) With increasing solvent polarity, there is a reduction in the intensity of the high-energy $S_1 \rightarrow S_n$ band (thick vertical line on the left-hand side of Figure 7) and an increase in the intensity of the $S_1 \rightarrow S_{n'}$ band (thin vertical line on the left-hand side of Figure 7) in the transient absorption spectra (Figure 6). With increasing solvent polarity, the $S_1 \rightarrow S_n$ band becomes weaker (thin vertical line on the right-hand side of Figure 7) in intensity and the $S_1 \rightarrow S_{n'}$ transition becomes more prominent (thick vertical line on the right-hand side of Figure 7). This happens because the presence of the CT component in the S_1 state shifts the global minimum of the potential energy surface and leads to a redistribution of the S_1 excited-state population. (2) With increasing solvent polarity there is a blue shift in the low-energy $S_1 \rightarrow S_{n'}$ band (thin vertical line on the left-hand side of Figure 7 and thick vertical line on the right-hand side of Figure 7). This is caused by the charge transfer component of the S_1 state responding to a polar solvent-induced interaction that decreases the energy of the potential energy minimum relative to the $S_{n'}$ state. (3) A shift to lower energy of the $S_1 \rightarrow S_0$ fluorescence with increasing solvent polarity (data not shown).[25] The change in the minimum of the potential energy surface causes a red shift of the fluorescence spectrum. (4) A reduction in the quantum yield of fluorescence.[25] (5) A decrease in the lifetime of the lowest excited state (Table 3).[25] These last two observations are consistent with enhanced internal conversion to the ground state from the lower energy S_1 state in the polar solvents. Overall, the strong coupling between the 2^1A_g and CT states has the effect of shifting the spectral line positions, altering the band intensities, and affecting the dynamics of the excited state depending on the solvent.

Peridinin shows the most pronounced effect of the solvent on its transient absorption spectrum and excited singlet state lifetime compared to the other carotenoids with carbonyl groups (Table 3 and Figure 6). The lack of a solvent dependence from neoxanthin shows that an allene group is not essential to observe these effects, but the presence of a carbonyl in conjugation with the π-electron system is. The results from uriolide acetate further support the conclusion that the solvent-induced effects do not depend solely on the presence of the allene. The results from fucoxanthin and spheroidenone show that the solvent-induced effects do require a carbonyl in conjugation. The reasons are obscure as to why spheroidenone shows an effect of the solvent on its steady-state and transient absorption spectra (Figure 6F), but not on its singlet-state lifetime (Table 3). These differences most likely result from variations in the electronic coupling in the different molecules. Indeed, fucoxanthin and uriolide acetate require a higher dielectric threshold than peridinin to effect a change in the dynamics of their lowest excited states (Figure 5).

The effect of the solvent environment on the spectroscopic properties and dynamics of the lowest excited singlet states of carbonyl-containing carotenoids is clearly demonstrated by this work and is providing an avenue to explore further the molecular factors controlling the photochemistry of these biologically important molecules both in vitro and in vivo.

Acknowledgment. We thank Professor Synnøve Liaaen-Jensen for the gift of the uriolide acetate and Professor Ron Christensen for helpful discussions. This work was supported by grants to H.A.F. from the National Institutes of Health (GM-30353), the National Science Foundation (MCB-9816759), and the University of Connecticut Research Foundation. The work at Argonne National Laboratory was supported by the Office of Basic Energy Sciences, Division of Chemical Sciences, U.S. Department of Energy, under Contract W-31-109-Eng-38. R.G.H was supported by Australian Research Council Grant A19600918.

References and Notes

(1) Christensen, R. L. In *The Photochemistry of Carotenoids*; Frank, H. A., Young, A. J., Britton, G., Cogdell, R. J., Eds.; Kluwer: Dordrecht, The Netherlands, 1999; pp 137−159.

(2) Krinsky, N. I. In *Carotenoids*; Isler, O., Ed.; Birkhäuser Verlag: Basel, 1971; pp 669−716.

(3) Frank, H. A.; Cogdell, R. J. In *Carotenoids in Photosynthesis*; Young, A., Britton, G., Eds.; Chapman and Hall: London, 1993; pp 252−326.
(4) Cogdell, R. J.; Frank, H. A. *Biochim. Biophys. Acta* **1987**, *895*, 63.
(5) Goodwin, T. W. *The Biochemistry of the Carotenoids*, 2nd ed.; Chapman & Hall: London, 1980; Vol. 1, p 220.
(6) Liaaen-Jensen, S. In *Carotenoids*; Britton, G., Liaaen-Jensen, S., Pfander, H., Eds.; Birkhäuser Verlag: Berlin, 1998; Vol. 3, p 217.
(7) Johansen, J. E.; Svec, W. A.; Liaaen-Jensen, S.; Haxo, F. T. *Phytochemistry* **1974**, *12*, 2261.
(8) Koka, P.; Song, P. *Biochim. Biophys. Acta* **1977**, *495*, 220.
(9) Bautista, J. A.; Hiller, R. G.; Sharples, F. P.; Gosztola, D.; Wasielewski, M.; Frank, H. A. *J. Phys. Chem. A* **1999**, *103*, 2267.
(10) Song, P.; Koka, P.; Prezelin, B.; Haxo, F. *Biochemistry* **1976**, *15*, 4422.
(11) Hofmann, E.; Wrench, P.; Diedrichs, K.; Sharples, F. P.; Hiller, R. G.; Welte, W.; Diedrichs, K. *Science* **1996**, *272*, 1788.
(12) Shreve, A. P.; Trautman, J. K.; Frank, H. A.; Owens, T. G.; van Beek, J. B.; Albrecht, A. C. *J. Lumin.* **1992**, *53*, 179.
(13) Katoh, T.; Nagashima, U.; Mimuro, M. *Photosynth. Res.* **1991**, *27*, 221.
(14) Akimoto, S.; Takaichi, S.; Ogata, T.; Nishimura, Y.; Yamazaki, I.; Mimuro, M. *Chem. Phys. Lett.* **1996**, *260*, 147.
(15) Liaaen-Jensen, S. *Carotenoids*; Britton, G.; Liaaen-Jensen, S.; Pfander, H., Eds.; Birkhäuser Verlag: Berlin, 1998; Vol. 3, p 217.
(16) Johansen, J. E.; Svec, W. A.; Liaaen-Jensen, S.; Haxo, F. T. *Phytochemistry* **1974**, *12*, 2261.
(17) Liaane-Jensen, S.; Jensen, A. *Methods Enzymol.* **1971**, *23*, 586.
(18) DeCoster, B.; Christensen, R. L.; Gebhard, R.; Lugtenburg, J.; Farhoosh, R.; Frank, H. A. *Biochim. Biophys. Acta* **1992**, *1102*, 107.
(19) Sashima, T.; Nagae, H.; Kuki, M.; Koyama, Y. *Chem. Phys. Lett.* **1999**, *299*, 187.
(20) Le Rosen, A. L.; Reid, C. E. *J. Chem. Phys.* **1952**, *20*, 233.
(21) Andersson, P. O.; Gillbro, T.; Ferguson, L.; Cogdell, R. J. *Photochem. Photobiol.* **1991**, *54*, 353.
(22) Nagae, H.; Kuki, M.; Cogdell, R. J.; Koyama, Y. *J. Chem. Phys.* **1994**, *101*, 6750.
(23) Basu, S. *Adv. Quantum Chem.* **1964**, *1*, 145.
(24) Hudson, B. S.; Kohler, B. E.; Schulten, K. In *Excited States*; Lim E. C., Ed.; Academic Press: New York, 1982; Vol. 6, pp 1−95.
(25) Bautista, J. A.; Connors, R. E.; Raju, B. B.; Hiller, R. G.; Sharples, F. P.; Gosztola, D.; Wasielewski, M. R.; Frank, H. A. *J. Phys. Chem. B* **1999**, *103*, 8751−8758.
(26) Rechthaler, K.; Köhler, G. *Chem. Phys.* **1994**, *189*, 99.
(27) Liaaen-Jensen, S. In *Carotenoid*; Isler, O.; Gutmann, H.; Solms, U., Eds.; Birkhäuser Verlag: Basel, 1971; p 163.
(28) Martinson, T. A.; Plumley, G. F. *Anal. Biochem.* **1995**, *228*, 123.
(29) Gosztola, D.; Yamada, H.; Wasielewski, M. R. *J. Am. Chem. Soc.* **1995**, *117*, 2041.
(30) Greenfield, S. R.; Wasielewski, M. R. *Opt. Lett.* **1995**, *20*, 1394.
(31) Microcal Software, Inc., One Roundhouse Plaza, Northampton, MA 01060.
(32) Hypercube, Inc., 1115 NW 4th St., Gainesville, FL 32601.
(33) Lakowicz, J. R. *Principles of Fluorescence Spectroscopy*; Plenum Press: New York and London, 1983; pp 67−70.
(34) Mimuro, M.; Nagashima, U.; Takaichi, S.; Nishimura, Y.; Yamazaki, I.; Katoh, T. *Biochim. Biophys. Acta* **1992**, *1098*, 271.
(35) Frank, H. A.; Desamero, R. Z. B.; Chynwat, V.; Gebhard, R.; van der Hoef, I.; Jansen, F. J.; Lugtenburg, J.; Gosztola, D.; Wasielewski, M. R. *J. Phys. Chem.* **1997**, *101*, 149.
(36) Strickler, S. J.; Berg, R. A. *J. Chem. Phys.* **1962**, *37*, 814.
(37) Hochstrasser, R. M.; Marzzacco, C. A. In *Molecular Luminescence*; Lim, E. C., Ed.; W. A. Benjamin, Inc.: New York, 1969; pp 631−656.
(38) Lim, E. C.; Yu, J. M. H. *J. Chem. Phys.* **1967**, *47*, 3270.
(39) Bublitz, G. U.; Ortiz, R.; Runser, C.; Fort, A.; Barzoukas, M.; Marder, S. R.; Boxer, S. G. *J. Am. Chem. Soc.* **1997**, *119*, 2311.
(40) Bublitz, G. U.; Ortiz, R.; Marder, S. R.; Boxer, S. G. *J. Am. Chem. Soc.* **1997**, *119*, 3365.
(41) Christensen, R. L.; Kohler, B. E. *Photochem. Photobiol.* **1973**, *18*, 293.
(42) Hemley, R.; Kohler, B. E. *Biophys. J.* **1977**, *20*, 377.
(43) Okada, T.; Mataga, N.; Baumann, W.; Siemiarczuk, A. J. *J. Phys. Chem.* **1987**, *91*, 4490.
(44) Rettig, W. *Angew. Chem., Int. Ed. Engl.* **1986**, *25*, 971.
(45) Frank, H. A.; Cua, A.; Chynwat, V.; Young, A.; Gosztola, D.; Wasielewski, M. R. *Photosynth. Res.* **1994**, *41*, 389.